

# Magnetic Properties of $\text{Yb}_2\text{Mo}_2\text{O}_7$ and $\text{Gd}_2\text{Mo}_2\text{O}_7$ from rare earth Mössbauer Measurements

J. A. Hodges, P. Bonville, A. Forget

*Commissariat à l'Energie Atomique, Centre d'Etudes de Saclay  
Service de Physique de l'Etat Condensé, 91191 Gif-sur-Yvette, France*

J. P. Sanchez, P. Vulliet

*Commissariat à l'Energie Atomique, Centre d'Etudes de Grenoble  
Service de Physique Statistique, Supraconductivité et Magnétisme, 38054 Grenoble, France*

M. Rams, K. Królas

*Institute of Physics, Jagiellonian University, 30-059 Kraków, Poland*

Using  $^{170}\text{Yb}$  and  $^{155}\text{Gd}$  Mössbauer measurements down to  $\sim 0.03\text{ K}$ , we have examined the semi-conducting pyrochlore  $\text{Yb}_2\text{Mo}_2\text{O}_7$  where the Mo intra-sublattice interaction is anti-ferromagnetic and the metallic pyrochlore  $\text{Gd}_2\text{Mo}_2\text{O}_7$  where this interaction is ferromagnetic. Additional information was obtained from susceptibility, magnetisation and  $^{172}\text{Yb}$  perturbed angular correlation measurements. The microscopic measurements evidence lattice disorder which is important in  $\text{Yb}_2\text{Mo}_2\text{O}_7$  and modest in  $\text{Gd}_2\text{Mo}_2\text{O}_7$ . Magnetic irreversibilities occur at 17 K in  $\text{Yb}_2\text{Mo}_2\text{O}_7$  and at 75 K in  $\text{Gd}_2\text{Mo}_2\text{O}_7$  and below these temperatures the rare earths carry magnetic moments which are induced through couplings with the Mo sublattice. In  $\text{Gd}_2\text{Mo}_2\text{O}_7$ , we observe the steady state Gd hyperfine populations at 0.027 K are out of thermal equilibrium, indicating that Gd and Mo spin fluctuations persist at very low temperatures. Frustration is thus operative in this essentially isotropic pyrochlore where the dominant Mo intra-sublattice interaction is ferromagnetic.

PACS numbers: 76.80+y, 75.50.Lk, 75.30-m

## I. INTRODUCTION

In the rare earth pyrochlores  $\text{R}_2\text{T}_2\text{O}_7$  (R is a trivalent rare earth, T a tetravalent transition or sp metal ion), each of the two cationic sublattices forms a network of corner sharing tetrahedra<sup>1,2</sup>. For this arrangement, each sublattice is prone to geometrically derived magnetic frustration<sup>3-5</sup>, with the behaviour in each particular compound depending on the sign, size and anisotropy of the interionic couplings. The main signatures of magnetic frustration are the absence of long range order and the persistence of dynamic short range magnetic correlations as  $T \rightarrow 0$ <sup>6</sup>.

The rare earth molybdates  $\text{R}_2\text{Mo}_2\text{O}_7$  may be formed with the rare earths from  $\text{Nd}^{3+}$  to  $\text{Lu}^{3+}$ <sup>1</sup>. For R from Nd to Gd, they show metallic-like behaviour, whereas for R from Dy to Lu (and with Y), they show semiconducting behaviour with an activation energy of the order of 15 meV<sup>2,7,8</sup>. The change in behaviour ("metal-semiconductor crossover") is chiefly linked with changes within the Mo-O subsystem and it has been related to variations in the Mo-O bond lengths associated with the changing lattice parameter (lanthanide contraction)<sup>9</sup> and in the Mo-O-Mo bond angles<sup>10</sup>. The metal-semiconductor crossover also leads to profound changes in the magnetic properties. In the semiconducting compounds, the Mo intra-sublattice coupling is antiferromagnetic<sup>11</sup>, whereas in the metallic compounds,

it is ferromagnetic<sup>8</sup>.

In the  $\text{R}_2\text{Mo}_2\text{O}_7$ , the dominant exchange interaction is that within the d-ion sublattice. The next most important interaction is the inter-sublattice exchange with the interaction within the f-ion sublattice the weakest of the three. For the d-ion sublattice, the dominant exchange mechanism is different either side of the metal-semiconductor crossover. In the semiconducting compounds, antiferromagnetic superexchange prevails whereas in the metallic compounds, the direct ferromagnetic coupling involving the Mo 4d-spin density at the Fermi level dominates<sup>12</sup>. An important feature controlling the properties of most of the  $\text{R}^{3+}$  ions and the way they are magnetised through coupling with the  $\text{Mo}^{4+}$  sublattice is the crystal field interaction, which fashions the wave functions of the  $\text{R}^{3+}$  ground state. This consideration does not concern the S-state  $\text{Gd}^{3+}$  ion which is essentially immune to the influence of crystal fields.

In  $\text{Y}_2\text{Mo}_2\text{O}_7$ , as in the other semiconducting molybdates, the Mo-Mo interaction is antiferromagnetic. A magnetic irreversibility occurs at 22 K evidencing a spin-glass-like transition<sup>11</sup>. This was a surprising result for a compound which seemed to be crystallographically ordered. Recent structural studies have shown, however, that the Mo-Mo (and some of the Y-O) bond lengths are disordered<sup>13</sup>, raising the possibility that the spin-glass-like transition is linked to the disorder and frustration.  $^{89}\text{Y}$  nuclear magnetic resonance measurements

have confirmed the presence of lattice disorder<sup>14</sup>. Magnetic frustration is clearly operative in  $\text{Y}_2\text{Mo}_2\text{O}_7$ : the spin fluctuations associated with the short range correlated Mo spins do not die out as  $T \rightarrow 0$ , but rather tend to a temperature independent rate<sup>15</sup> and neutron scattering measurements have shown that the spin-glass-like transition occurs mainly in the frequency domain<sup>16</sup>. In  $\text{Gd}_2\text{Mo}_2\text{O}_7$ , as in the other metallic molybdates, the Mo-Mo interaction is ferromagnetic. A transition occurs with a temperature that depends on the sample ( $T_C \simeq 55\text{ K}$  in Refs. 8, 17 and  $\simeq 65\text{ K}$  in Ref. 9), and it is accompanied by a magnetic irreversibility. Little information is available concerning the possible influence of frustration in this compound although specific heat measurements down to  $\sim 1.8\text{ K}$  have suggested that the low energy tail of the density of magnetic excitations does not tend to zero<sup>17</sup>.

We present a study of semiconducting  $\text{Yb}_2\text{Mo}_2\text{O}_7$  and metallic  $\text{Gd}_2\text{Mo}_2\text{O}_7$  based chiefly on rare earth Mössbauer measurements (respectively using the isotopes  $^{170}\text{Yb}$  and  $^{155}\text{Gd}$ ) down to  $\sim 30\text{ mK}$ . Magnetic measurements were also made for the two compounds, and  $^{172}\text{Yb}$  perturbed angular correlation (PAC) were carried out for  $\text{Yb}_2\text{Mo}_2\text{O}_7$  up to  $\sim 1000\text{ K}$ . We obtain information concerning the static and dynamic magnetic properties of the rare earths and concerning the ordering and spin-dynamics of the  $\text{Mo}^{4+}$  sub-lattice and its coupling with the  $\text{R}^{3+}$  sublattices. Making use of the microscopic nature of the Mössbauer probes, we discuss the information obtained concerning local symmetry lowering and bond disorder in the two compounds, which are *a priori* expected to be crystallographically ordered.

After outlining some background properties of the two samples in section II, we present the results concerning  $\text{Yb}_2\text{Mo}_2\text{O}_7$  in section III and concerning  $\text{Gd}_2\text{Mo}_2\text{O}_7$  in section IV. Section V contains the summary and discussion.

## II. SAMPLES AND BACKGROUND RARE EARTH SINGLE ION PROPERTIES.

The polycrystalline samples of  $\text{Yb}_2\text{Mo}_2\text{O}_7$  and  $\text{Gd}_2\text{Mo}_2\text{O}_7$  were prepared by first reacting Mo and  $\text{MoO}_3$  in a sealed container to form  $\text{MoO}_2$  which was then reacted under argon with the  $\text{R}_2\text{O}_3$ . Room temperature X-ray diffraction measurements show both samples are single phase and provide the cubic lattice parameter:  $10.146\text{ Å}$  ( $\text{Yb}_2\text{Mo}_2\text{O}_7$ ) and  $10.366\text{ Å}$  ( $\text{Gd}_2\text{Mo}_2\text{O}_7$ ).

The cubic pyrochlore structure (space group  $\text{Fd}\bar{3}\text{m}$ ) contains eight formula units per unit cell. The  $\text{R}^{3+}$  ions situated at the 16b sites (point symmetry:  $\bar{3}\text{m}$ ), form a network of corner sharing tetrahedra. Each of the four  $\text{R}^{3+}$  making up a tetrahedron has its local symmetry axis along one of the  $[111]$  directions. The  $\text{Mo}^{4+}$  situated at the 16d sites (point symmetry:  $\bar{3}\text{m}$ ), also form a network of corner sharing tetrahedra which is displaced by  $(1/2, 1/2, 1/2)$  relative to that of the  $\text{R}^{3+}$ .

$\text{Yb}^{3+}$  ( $4f^{13}$ ) has 8 sublevels in its spin-orbit derived ground state ( $^2\text{F}_{7/2}$ ). The degeneracy is partially lifted by the crystal electric field to leave four Kramers doublets. In an isomorphous pyrochlore ( $\text{Yb}_2\text{Ti}_2\text{O}_7$ ), the total energy separation of the four doublets is about  $1000\text{ K}$  and the well isolated ground state Kramers doublet has planar anisotropy with the easy magnetisation plane lying perpendicular to the appropriate local  $[111]$  direction<sup>20</sup>.

$\text{Gd}^{3+}$  ( $4f^7$ ) is an S-state ion ( $^8\text{S}_{7/2}$ ). Both its anisotropy and the amount of crystal field degeneracy lifting within the 8 sublevels of the ground state are quite small. In the context of the present study, this ground state can be taken to be an initially degenerate  $S=7/2$  state, whose degeneracy is lifted only by a molecular or applied magnetic field.

## III. $\text{Yb}_2\text{Mo}_2\text{O}_7$

### A. Susceptibility and magnetisation measurements.

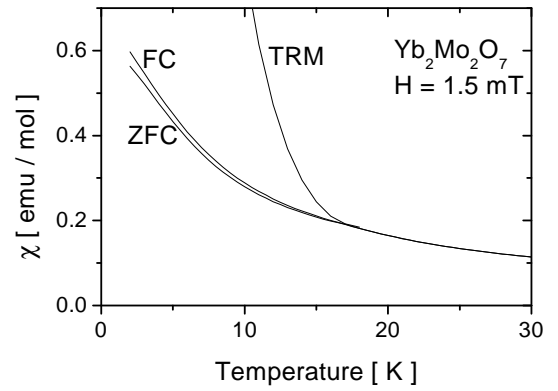


FIG. 1. Magnetic susceptibility of  $\text{Yb}_2\text{Mo}_2\text{O}_7$  with an applied field of  $1.5\text{ mT}$  in the field cooled (FC), zero field cooled (ZFC) and thermo-remnant magnetisation (TRM) configurations. The use of the TRM dependence (which was scaled to fit the figure) provides a more accurate assessment of the irreversibility temperature ( $17\text{ K}$ ).

The magnetic susceptibility of  $\text{Yb}_2\text{Mo}_2\text{O}_7$  was measured from  $300$  to  $2\text{ K}$ . Both the field cooled (FC) and zero field cooled (ZFC) variations change monotonically as the temperature is lowered and there is a small irreversibility with an onset in the range  $16 - 18\text{ K}$  (Fig.1).

To obtain a more accurate value for the irreversibility temperature  $T_{irr}$ , we measured the thermo-remnant magnetisation (TRM) after field cooling with  $5\text{ T}$  down to  $2\text{ K}$  (Fig.1). We then obtain  $T_{irr} = 17.0\text{ K}$ . The size of the low field irreversibility as evidenced by the difference between the the FC and ZFC branches, is quite small and it is somewhat different to that observed in  $\text{Y}_2\text{Mo}_2\text{O}_7$ <sup>11</sup>. The question then arises as to the nature of the transition occurring at  $T_{irr}$ . We first note

that cases are known where antiferromagnetic (AF) ordering takes place without giving rise to an anomaly in the magnetic susceptibility (see for instance, Ref. 18 for the case of the Yb pnictides). Thus, the fact that there is no strong anomaly does not in itself represent evidence against the existence of low temperature magnetic order or correlations. In fact, as is described in section III B, at temperatures below  $T_{irr}$ , the  $^{170}\text{Yb}$  Mössbauer data evidence  $\text{Yb}^{3+}$  magnetic hyperfine fields and  $\text{Yb}^{3+}$  magnetic moments which are produced through Mo-Yb exchange.  $T_{irr}$  could then correspond to a change in the length scale and/or in the fluctuation rate of the correlations within the Mo sublattice.

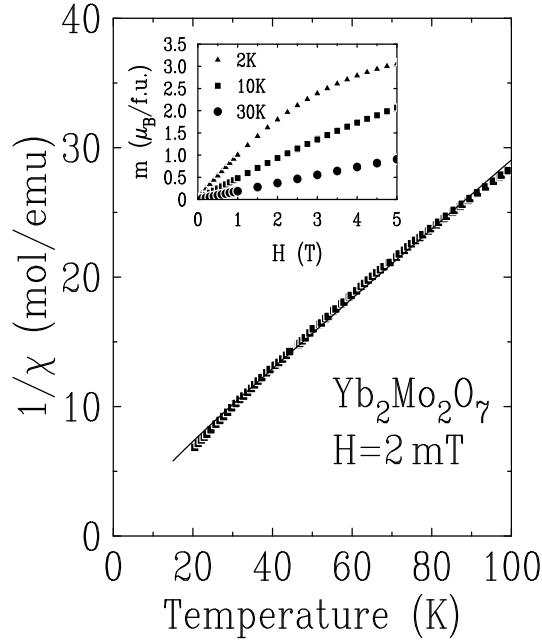


FIG. 2. Inverse magnetic susceptibility in  $\text{Yb}_2\text{Mo}_2\text{O}_7$  with a field of 2 mT; the solid line is a fit as explained in the text. Inset: field dependence of the isothermal magnetisation per formula unit at selected temperatures.

The value of  $T_{irr}$  can be linked to one of two possible scenarios. First, that frustration does not play a major role so that  $T_{irr}$  directly corresponds to the strength of the molecular field interaction within the  $\text{Mo}^{4+}$  sublattice. Second, that frustration is operative and in common with the typical behaviour of frustrated compounds, the temperature of the transition ( $T_{irr}$ ) is much smaller than the temperature equivalent to the strength of the Mo-Mo coupling. We examine the two possibilities in turn. For the first case, we analyse the inverse susceptibility  $1/\chi$  between 20-100 K (Fig.2) in terms of the molecular field approximation. In this temperature range,  $1/\chi$  shows a quasi-linear thermal dependence, with a small background curvature due to the influence of the three  $\text{Yb}^{3+}$  Kramers doublet excited crystal field levels which have energies up to  $\sim 1000$  K (see section III C). Below 100 K, only the ground crystal field  $\text{Yb}^{3+}$  doublet is apprecia-

bly populated and it is described by an effective spin 1/2 and a crystal field derived spectroscopic g-tensor. As  $\text{Yb}_2\text{Mo}_2\text{O}_7$  is an insulator, an ionic description for the  $\text{Mo}^{4+}$  ion, *i.e.*  $S=1$  and a g-factor close to 2, should be adequate. We assume the following hierarchy of exchange interactions: a dominant Mo-Mo coupling which is AF and a smaller Mo-Yb exchange, with a molecular field constant  $\lambda$ . For a two magnetic sublattice system in the paramagnetic region, the molecular field theory leads to a ferrimagnetic-like inverse susceptibility:

$$\frac{1}{\chi} = \frac{T(T + T_N) - \lambda^2 C_{\text{Mo}} C_{\text{Yb}}}{T(C_{\text{Mo}} + C_{\text{Yb}}) + 2\lambda C_{\text{Mo}} C_{\text{Yb}} + C_{\text{Yb}} T_N}, \quad (1)$$

where  $C_{\text{Mo}}$  and  $C_{\text{Yb}}$  are the Curie constants respectively of  $\text{Mo}^{4+}$  and  $\text{Yb}^{3+}$ . Setting  $T_N = T_{irr} = 17$  K, expression (1) reproduces the main features of the thermal variation of  $1/\chi$  (solid line in Fig.2) with a  $\text{Mo}^{4+}$  g-value of 1.9(1) (close to the ionic value appropriate for a high spin  $\text{Mo}^{4+}$  ion) and an average  $\text{Yb}^{3+}$  g-value of 3.2(2). This latter value is coherent with the average saturated magnetic moment of  $1.7 \mu_B$  measured by  $^{170}\text{Yb}$  Mössbauer spectroscopy (see section III B). The Mo-Yb exchange constant  $\lambda$  derived from this analysis is antiferromagnetic, and its value lies in the range from  $-0.82$  to  $-2.20$  T/ $\mu_B$ . This yields a mean saturated molecular field acting on the  $\text{Yb}^{3+}$  ion of 2.75 T and a mean Yb-Mo exchange energy of about 3 K. In agreement with this analysis, the direct extrapolation of the inverse susceptibility (Fig.2) leads to a paramagnetic Curie-Weiss temperature with a value in the range -5 to -10 K (AF interaction). The AF nature of the correlations is confirmed by two aspects of the magnetisation measurements which are shown in the inset of Fig.2 : the increase of the moment with applied field is relatively slow and at 2 K, saturation is not achieved in a field of 5 T.

The possibility that the strength of the Mo - Mo sublattice interaction is very much bigger than that corresponding to  $T_{irr}$  is based, for the moment, only on the analogy with the situation in  $\text{Y}_2\text{Mo}_2\text{O}_7$ . In this case, muon spin relaxation ( $\mu\text{SR}$ )<sup>15</sup>, neutron diffraction<sup>16</sup> and unpublished high temperature susceptibility measurements quoted in Ref. 16 all point to the presence of a Mo - Mo interaction which is much bigger than that corresponding to  $T_{irr}$ . It is not feasible to access the Mo - Mo interaction in  $\text{Yb}_2\text{Mo}_2\text{O}_7$  from high temperature susceptibility measurements because of the temperature dependent contribution coming from the  $\text{Yb}^{3+}$  excited crystal field levels. To our knowledge, no  $\mu\text{SR}$  or neutron diffraction measurements have yet been carried out on  $\text{Yb}_2\text{Mo}_2\text{O}_7$ .

## B. $^{170}\text{Yb}$ Mössbauer measurements.

The  $^{170}\text{Yb}$  Mössbauer absorption measurements were made over the temperature range 95 to 0.036 K using a source of  $\text{Tm}^*\text{B}_{12}$  and a triangular velocity sweep. For

$^{170}\text{Yb}$ , the ground nuclear state has a spin  $I_g = 0$ , the excited nuclear state has a spin  $I_{ex} = 2$  and a quadrupole moment  $Q = -2.11\text{ b}$ , and  $E_\gamma = 84.3\text{ keV}$  and  $1\text{ cm/s}$  corresponds to  $680\text{ MHz}$ .

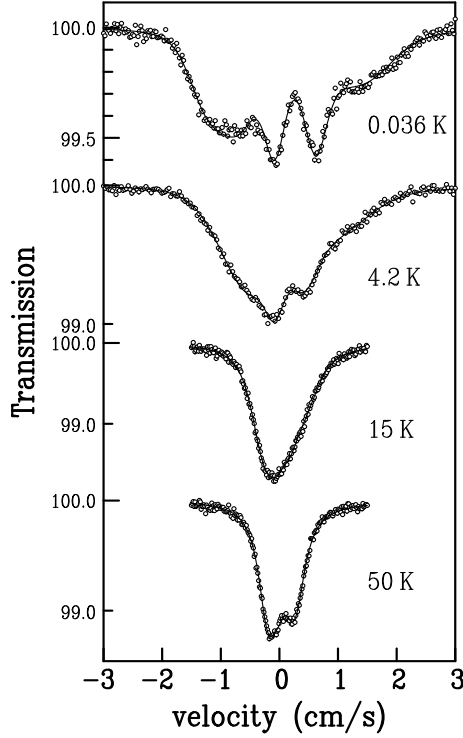


FIG. 3.  $^{170}\text{Yb}$  Mössbauer absorption spectra for  $\text{Yb}_2\text{Mo}_2\text{O}_7$ . At 50 K, only a quadrupole hyperfine interaction is present. To obtain the satisfactory linefit shown, it is necessary to allow this interaction to show a distribution and to introduce an asymmetry parameter. At the three lower temperatures an additional magnetic hyperfine interaction is also present.

In the upper part of the examined temperature range, the spectra are well described in terms of quadrupole hyperfine interactions, showing that in this region, the  $\text{Yb}^{3+}$  ions are paramagnetic. As exemplified by the data at 50 K on Fig. 3, we find that an acceptable data fit cannot be obtained if the quadrupole hyperfine interaction is taken to have the axial symmetry that is characteristic of the rare earth site in the standard pyrochlore structure. To obtain a good quality data fit, it is necessary both to introduce an asymmetry parameter ( $\eta$ ) and to allow the principal component  $V_{ZZ}$  of the electric field gradient tensor to show a distribution. We find  $\eta = 0.6$  and with a Gaussian shaped distribution, we obtain a mean value:  $eQV_{ZZ}/8 = 1.3\text{ mm/s}$  and a root mean square deviation:  $\sigma \simeq 0.4\text{ mm/s}$ . The microscopic Mössbauer probe measurements thus identify two aspects of the local structure of  $\text{Yb}_2\text{Mo}_2\text{O}_7$ : the point symmetry at the Yb site is non-axial and there is a distribution of environments indicating that significant disorder is present.

Lattice disorder has previously been evidenced in the iso-morphous semiconducting compound  $\text{Y}_2\text{Mo}_2\text{O}_7$  by X-ray absorption edge<sup>13</sup> and  $^{89}\text{Y}$  nuclear magnetic resonance<sup>14</sup> measurements. There was no evidence of any significant departure from full oxygen stoichiometry nor of site exchange and it was suggested that the disorder principally involved the Mo-Mo pair distances with also some modest disorder in the Y-O(1) distances<sup>13</sup>. It seems likely that an analogous situation will also pertain in  $\text{Yb}_2\text{Mo}_2\text{O}_7$  and that the anomalous characteristics of the quadrupole hyperfine interaction reported here are linked to lattice disorder involving some of the bond lengths and angles.

At low temperatures, magnetic hyperfine splittings are visible (Fig.3). Such splittings appear when the  $\text{Yb}^{3+}$  moments are either long or short range magnetically correlated and when any fluctuation of the correlated moments occurs at frequencies of the order of or below the  $^{170}\text{Yb}$  Mössbauer threshold value  $\sim 3.0 \times 10^8\text{ s}^{-1}$ . We first consider the data at 0.036 K. The overall shape of the spectrum and in particular the inhomogeneous broadenings of the 5 lines, point to the presence of a distribution in hyperfine field and quadrupolar coupling parameter values. This is coherent with the analysis of the data in the paramagnetic region, which evidenced a distribution of quadrupole hyperfine interactions. Both distributions can be linked to distribution in the  $\text{Yb}^{3+}$  ground state wave functions which results from the local disorder. In presence of random disorder, it can be shown that the distributions in the hyperfine field and quadrupolar parameters are linearly correlated<sup>19</sup>. Using linearly correlated distributions, we obtain good data fits (Fig.3) and these provide the mean  $^{170}\text{Yb}$  hyperfine field and the root mean square deviation of the distribution. The saturated values at 0.036 K are respectively 175 T and 45 T. The mean saturated  $\text{Yb}^{3+}$  magnetic moment value is therefore  $1.7\mu_B$ , using the standard  $^{170}\text{Yb}^{3+}$  relation:  $1\mu_B$  corresponds to 102 T.

The spectra become less resolved as the temperature increases (Fig.3). Reliable fits in terms of a distribution of hyperfine fields are possible only up to 10 K. The thermal variation of the mean  $\text{Yb}^{3+}$  moment is shown on Fig.4. The theoretical curve is obtained assuming that the  $\text{Yb}^{3+}$  ground doublet, with effective spin 1/2 and spectroscopic factor  $g$ , is polarised by the molecular field  $H_{ex}$  due to Mo-Yb exchange. In order to calculate  $H_{ex}(T)$ , which is proportional to the Mo moment within a molecular field model, we assume that the thermal variation of the Mo moment follows the mean field law for  $S=1$ . Then the reduced exchange field  $\sigma(T) = H_{ex}(T)/H_{ex}(0)$  is obtained by solving the self-consistent equation:

$$\sigma(T) = \mathcal{B}_1 \left( \frac{3S}{S+1} \frac{\sigma(T)}{\tau} \right), \quad (2)$$

where  $\mathcal{B}_1$  is the Brillouin function for  $S = 1$  and  $\tau = T/T_N$ . The solid line in Fig.4 is obtained with  $T_N = 17\text{ K}$  and  $H_{ex}(0) = 3\text{ T}$ , corresponding to an exchange energy of 3.4 K. This value is in good agreement with

that derived from the analysis of the susceptibility data (section III A).

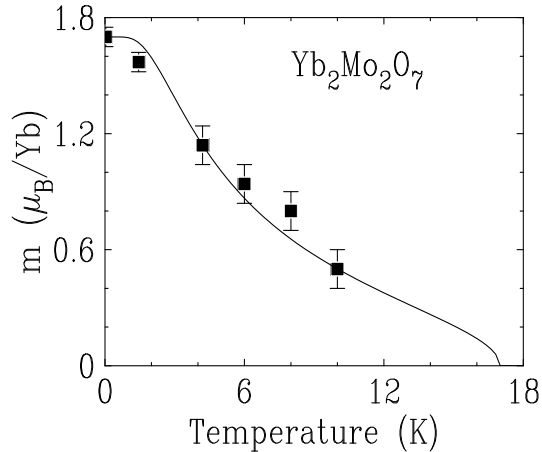


FIG. 4. Thermal dependence of the mean  $\text{Yb}^{3+}$  magnetic moment in  $\text{Yb}_2\text{Mo}_2\text{O}_7$  obtained from  $^{170}\text{Yb}$  Mössbauer measurements. The solid line is a fit to a molecular field model as explained in the text.

Although no reliable values can be obtained for the hyperfine field as the temperature is increased above  $\sim 10\text{ K}$ , it is clear that correlated  $\text{Yb}^{3+}$  magnetic moments are still present. In fact, the lineshapes also show that some correlations persists above  $17\text{ K}$ . Both just above and just below the irreversibility temperature, the Mössbauer line shapes are compatible with the presence of dynamic magnetic correlations.

### C. $^{172}\text{Yb}$ perturbed angular correlation (PAC) measurements.

The PAC measurements provide the thermal dependence of the absolute value of the quadrupole hyperfine interaction at the  $^{172}\text{Yb}$  nucleus<sup>20,21</sup>. They were made over the range  $34$  to  $965\text{ K}$ , that is at temperatures above the range where magnetic correlations are present. Three examples of the spectra are shown in Fig. 5.

The strong damping of the  $R(t)$  oscillations visible in Fig. 5 is very characteristic of a hyperfine interaction which is distributed in size. The spectra cannot be fitted in terms of a single quadrupole interaction at any temperature and it is necessary to allow for a distribution of the fitted electric field gradient. This observation reinforces the same conclusion obtained from the  $^{170}\text{Yb}$  Mössbauer analysis.

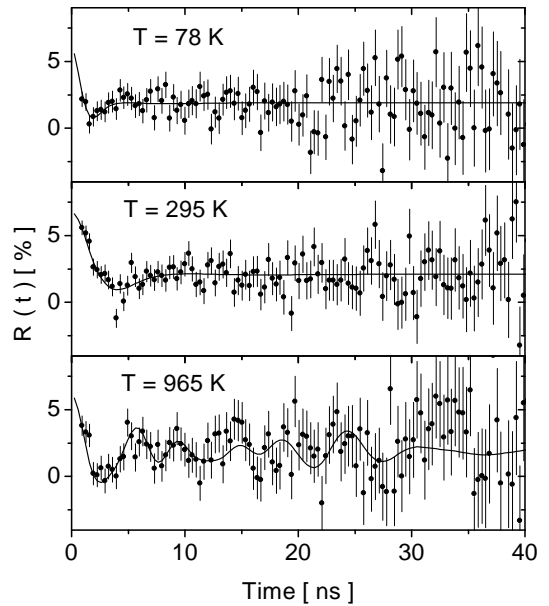


FIG. 5.  $^{172}\text{Yb}$  perturbed angular correlation spectra for  $\text{Yb}_2\text{Mo}_2\text{O}_7$ . The solid lines show the fitted perturbation factor due to a distribution of electric quadrupolar interactions in the  $I = 3$  intermediate level.

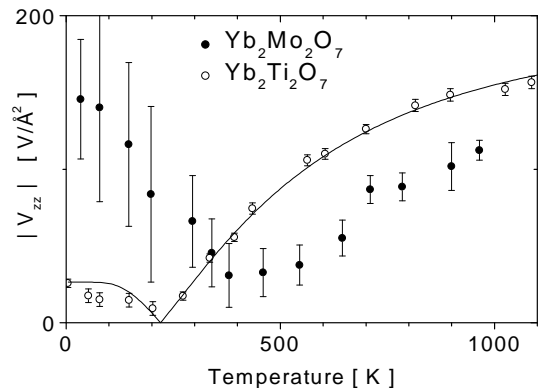


FIG. 6. Full points: thermal dependence of the absolute size of the principal component  $V_{ZZ}$  of the electric field gradient tensor in  $\text{Yb}_2\text{Mo}_2\text{O}_7$  obtained from  $^{172}\text{Yb}$  perturbed angular correlation measurements. At all temperatures  $V_{ZZ}$  shows a distribution which is more important at low temperatures than at high temperature, the root mean squares of the Gaussian are shown by the vertical bars. Open points: corresponding results (from Ref. 20) obtained in  $\text{Yb}_2\text{Ti}_2\text{O}_7$  where essentially no distribution is observed and where the vertical bars correspond to the experimental error; the solid line was calculated using a crystal field model.

It turns out that in presence of this distribution, the PAC data are not very sensitive to the asymmetry parameter  $\eta$ . The PAC technique thus cannot provide independent evidence confirming the conclusion of the  $^{170}\text{Yb}$  Mössbauer analysis that this parameter is non-zero. The thermal variation of the mean absolute value of  $V_{ZZ}$  and

of  $\sigma$  the width of its Gaussian distribution are shown in Fig. 6. The total interaction is made up of two parts, one which is temperature dependent arising from the  $\text{Yb}^{3+}$  4f shell, and one which is essentially temperature independent arising from the lattice charges. At low temperatures, the 4f electron contribution dominates whereas at high temperatures, the total 4f contribution tends to zero and the lattice contribution dominates.

At the lowest measurement temperature, the mean value for  $|V_{ZZ}|$  agrees with that obtained from the  $^{170}\text{Yb}$  Mössbauer analysis. This latter technique also provides the sign of the gradient showing that in the low temperature limit  $V_{ZZ} = -135 \text{ V}/\text{\AA}^2$ . The two techniques also provide essentially the same value for  $\sigma$ , the root mean square deviation of the distribution.

As shown on Fig.6, the electric field gradient also evidences a distribution in the high temperature region of the measurement range. Since the electric field gradient in this region is due chiefly to the surrounding lattice charges, the observation of a distribution directly evidences the presence of lattice disorder. We attribute the fact that the size of the distribution of the electric field gradient is much bigger at low temperatures to the fact that the disorder gives rise to a distribution in the  $\text{Yb}^{3+}$  crystal field parameters and wave functions and this leads to an enhanced distribution in the part of the quadrupolar hyperfine interaction linked with the 4f-shell.

Because of the local symmetry lowering, it is impossible to carry out a crystal field analysis of the thermal variation of  $V_{ZZ}$ , such as was done for  $\text{Yb}_2\text{Ti}_2\text{O}_7$ <sup>20</sup>. The values for this latter compound, also shown in Fig.6, are different from those in  $\text{Yb}_2\text{Mo}_2\text{O}_7$  showing there are some differences between the  $\text{Yb}^{3+}$  crystal field properties of the two compounds. The temperature range over which the gradient continues to vary is however similar in the two cases suggesting the overall crystal field splittings are of comparable magnitudes ( $\sim 1000 \text{ K}$ ) in the two compounds.

#### IV. $\text{Gd}_2\text{Mo}_2\text{O}_7$ .

##### A. Susceptibility and magnetisation measurements.

The magnetic susceptibility  $\chi(T)$  and magnetisation  $m(H)$  measurements are shown in Fig.7. The sharp rise in  $\chi(T)$  that occurs at  $\sim 80 \text{ K}$  (previously observed at  $\sim 55 \text{ K}$ <sup>8,17</sup> and at  $\sim 65 \text{ K}$ <sup>9</sup>) suggests the onset of ferromagnetic ordering of the  $\text{Mo}^{4+}$  moments. The specific heat shows only a broad anomaly near the temperature of the susceptibility rise,<sup>17</sup> suggesting the ordering is short range. An irreversibility between the FC and ZFC branches (reported previously<sup>8,17</sup>) is observed below  $75 \text{ K}$ . It is probably chiefly related to the pinning of domain walls by defects.

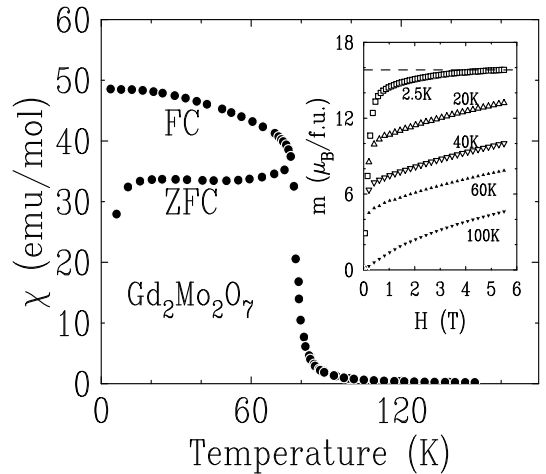


FIG. 7. Magnetic susceptibility of  $\text{Gd}_2\text{Mo}_2\text{O}_7$  with an applied field of  $0.2 \text{ mT}$ . FC: field cooled and ZFC: zero field cooled. **Inset:** isothermal magnetisation curves at selected temperatures.

The rapid initial rise of the magnetisation curves (inset of Fig.7) measured below  $60 \text{ K}$  also evidences ferromagnetic interactions. At  $2.5 \text{ K}$ , the quasi-saturated value of the high field magnetisation of  $15.8(4) \mu_B$  per formula unit (dashed line in the inset of Fig.7) shows the Gd-Mo coupling is ferromagnetic. The two  $\text{Gd}^{3+}$  ions contribute a saturated moment of  $14 \mu_B$ , and thus each  $\text{Mo}^{4+}$  ion carries a moment of  $0.9(2) \mu_B$ , parallel to that of the  $\text{Gd}^{3+}$ , as reported previously<sup>2</sup>. This value for the  $\text{Mo}^{4+}$  moment is much smaller than that expected assuming an ionic description in terms of high spin  $4d^2$ ,  $t_{2g}$  state with  $S=1$  and  $g \sim 2$  ( $\sim 2 \mu_B$ ). Furthermore, our attempts to fit the magnetisation curves within a self-consistent molecular field model assuming an ionic description for  $\text{Mo}^{4+}$  as well as for  $\text{Gd}^{3+}$  failed even allowing the Mo g-factor to be adjustable. The magnetic properties of the Mo in metallic  $\text{Gd}_2\text{Mo}_2\text{O}_7$  thus appear to be associated rather with exchange coupled 4d electrons with some metallic character.

##### B. $^{155}\text{Gd}$ Mössbauer measurements.

The  $^{155}\text{Gd}$  Mössbauer absorption measurements were made over the temperature range  $80$  to  $0.027 \text{ K}$  using a source of  $\text{Sm}^*\text{Pd}_3$ . The isotope  $^{155}\text{Gd}$  has a ground nuclear state with spin  $I_g = 3/2$  and quadrupole moment  $Q=1.31 \text{ barn}$ , and an excited nuclear state with spin  $I_{ex} = 5/2$  and very small quadrupole moment. The transition energy is  $E_\gamma = 86.5 \text{ keV}$ , and  $1 \text{ mm/s}$  corresponds to  $69.8 \text{ MHz}$ . Spectra at some selected temperatures are shown in Fig. 8.

At  $80 \text{ K}$ , in the paramagnetic phase, the absorption takes the form of a nearly symmetric doublet. It corresponds to a quadrupole hyperfine interaction, with a quadrupolar splitting  $\frac{eQV_{ZZ}}{2}(1 + \frac{\eta^2}{3})^{1/2} \simeq -5.1 \text{ mm/s}$

(the negative sign is obtained from the analysis of the line shapes at low temperatures when a hyperfine field is also present and  $\eta$  is included to allow for possible local symmetry lowering). For the S-state  $\text{Gd}^{3+}$  ion, the quadrupole hyperfine interaction is due only to the neighbouring lattice charges. As in other Gd pyrochlores<sup>22</sup>, the interaction is quite large in keeping with the important local structural anisotropy of the rare earth site.

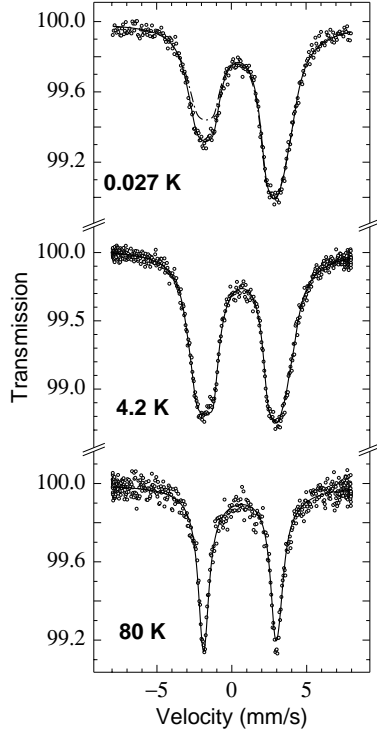


FIG. 8.  $^{155}\text{Gd}$  Mössbauer absorption spectra for  $\text{Gd}_2\text{Mo}_2\text{O}_7$ . The two data fits (full and dashed lines) shown at 27 mK are discussed in the text in relation to the presence of out of equilibrium hyperfine level populations.

A hyperfine field, proportional to the  $\text{Gd}^{3+}$  moment, appears when the temperature is lowered below  $\sim 75$  K, and this confirms the magnetic transition evidenced by the susceptibility data. In  $\text{Gd}_2\text{Mo}_2\text{O}_7$ , the magnetic hyperfine interaction is much smaller than the quadrupole interaction, and the hyperfine field acts only to broaden each of the two absorption lines. At 0.027 K, the saturated hyperfine field is:  $H_{hf}(0) \simeq 19.8$  T, which is markedly smaller than that usually found in insulating Gd compounds ( $\sim 30$  T). The reduced value of  $H_{hf}(0)$  in this metallic compound is probably linked to the exchange polarisation of  $s$ -type conduction electrons, which contributes a hyperfine field opposite to that arising from the polarisation of the core  $s$ -electrons by the 4f shell moment. At 0.027 K, the relative intensity of the two absorption lines is different from that at 4.2 K even though the value of the hyperfine field remains essentially the same. The change in the relative intensity at very low

temperatures is related to changes in the populations of the sublevels of the  $^{155}\text{Gd}$  nuclear ground state and these will be discussed at more length in section IV C.

The asymmetry parameter of the electric field gradient tensor ( $\eta$ ) can only be obtained from a  $^{155}\text{Gd}$  Mössbauer measurement when a magnetic hyperfine interaction is present. From the 0.027 K spectrum, we obtain  $0.0 \leq \eta \leq 0.4$ . Thus, although it is possible that  $\eta$  is zero as expected for the axially symmetric rare earth site of the standard pyrochlore structure, we cannot discount the possibility (clearly established above for  $\text{Yb}_2\text{Mo}_2\text{O}_7$ ) that  $\eta$  is not exactly zero in which case local symmetry lowering is present. Over the whole temperature range, *i.e.*, in both the paramagnetic and magnetically correlated regions, we find the line widths of the individual transitions are  $\sim 20\%$  larger than in the compound  $\text{Gd}_2\text{Sn}_2\text{O}_7$  where  $\eta$  is essentially zero<sup>24</sup>. We attribute the background line broadening in  $\text{Gd}_2\text{Mo}_2\text{O}_7$  to indicate the quadrupolar hyperfine interaction shows a small distribution. Since this interaction arises solely from the electric field gradient created by the lattice charges, the presence of a distribution directly provides evidence for local disorder.

In principle, the analysis of the Mössbauer absorption provides the angle  $\theta$  between the direction of the magnetic moment and the principal local axis of the electric field gradient tensor (a [111] direction). The best fit yielded  $\theta \simeq 55^\circ$  but only marginally poorer quality fits were obtained if  $\theta$  was assumed to be distributed at random. The reduced sensitivity of the data fits to the direction of the hyperfine field is linked to the fact that the magnetic hyperfine interaction is much smaller than the quadrupole hyperfine interaction. Since the  $\text{Gd}^{3+}$  ion is essentially isotropic, the direction of the hyperfine field corresponds to the direction of the exchange field coming from the  $\text{Mo}^{4+}$  sublattice. The choice of a unique angle  $\theta \simeq 55^\circ$  is compatible with a magnetic structure where the  $\text{Gd}^{3+}$  and the  $\text{Mo}^{4+}$  moments are both aligned close to a [100] axis. To our knowledge,  $\text{Gd}_2\text{Mo}_2\text{O}_7$  has not been studied by neutron diffraction. Such measurements are, in fact, difficult due to the high neutron absorption cross section of non-enriched Gd. They would be useful in order to check if the moments are aligned towards a [100] direction and also, in fact, to establish whether the magnetic correlations are short or long range. We recall that a specific heat analysis in  $\text{Gd}_2\text{Mo}_2\text{O}_7$  suggested that there is no long range order<sup>17</sup> and that in  $\text{Nd}_2\text{Mo}_2\text{O}_7$ , which is also metallic, neutron diffraction measurements showed the magnetic order is long range<sup>23</sup> and the ferromagnetically coupled  $\text{Mo}^{4+}$  moments are aligned close (from  $6$  to  $9^\circ$ ) to a [100] direction.

In their analysis of the magnetic specific heat in  $\text{Gd}_2\text{Mo}_2\text{O}_7$ , the authors of Ref. 17 assume that even at very low temperatures, the exchange field experienced by the  $\text{Gd}^{3+}$  ion is distributed in size, with a finite weight at zero field. We tried to check this assumption by simulating spectra with such a distribution but no clear conclusion could be reached.

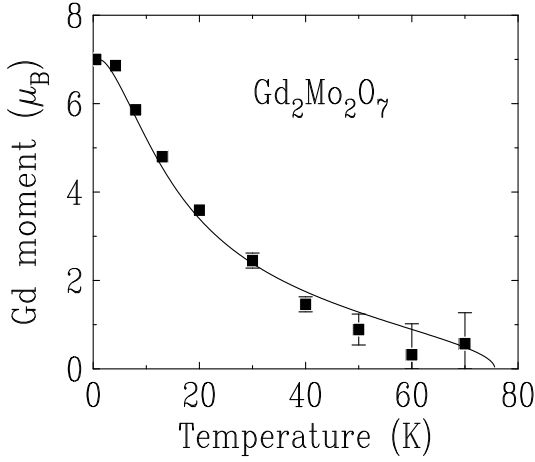


FIG. 9. Thermal variation of the  $\text{Gd}^{3+}$  4f shell magnetic moment in  $\text{Gd}_2\text{Mo}_2\text{O}_7$  obtained from  $^{155}\text{Gd}$  Mössbauer measurements. The solid line is a fit with the molecular field model described in the text.

Fig.9 shows the thermal variation of the  $\text{Gd}^{3+}$  4f shell magnetic moment, obtained from the hyperfine field value by scaling, using the relation that the measured saturated hyperfine field of 19.8 T corresponds to a saturated  $\text{Gd}^{3+}$  moment of  $7 \mu_B$ . In order to analyse these data, we assume the usual hierarchy of exchange interactions, in decreasing order: Mo-Mo, responsible for the transition at 75 K, Mo-Gd, responsible for the  $\text{Gd}^{3+}$  polarisation below 75 K, and Gd-Gd, which we will neglect here. Then, the  $\text{Gd}^{3+}$  magnetic moment at a temperature  $T$  is given by:

$$M_{\text{Gd}}(T) = M_{\text{Gd}}(0) \mathcal{B}_{7/2} \left( \frac{M_{\text{Gd}}(0) H_{\text{ex}}(T)}{k_B T} \right), \quad (3)$$

where  $\mathcal{B}_{7/2}$  is the Brillouin function for  $S = 7/2$  and  $H_{\text{ex}}(T)$  is the Mo derived exchange field which is obtained by solving Eqn.2 with  $\tau = T/T_C$  and  $T_C = 75$  K, the  $\text{Mo}^{4+}$  ordering temperature. The solid line on Fig.9, which provides a good fit to the experimental data, is obtained with a Mo-Gd exchange field  $H_{\text{ex}}(0) = 5.5$  T. The Mo-Gd exchange energy can then be estimated as:  $E_{\text{ex}} = M_{\text{Gd}}(0) H_{\text{ex}}(0) \simeq 26$  K. This is smaller than  $T_C$  and so *a posteriori* justifies the approximations made in the above calculation. The mean size of the  $\text{Mo}^{4+}$  derived field acting on the  $\text{Gd}^{3+}$  obtained here is  $\sim 30\%$  lower than that estimated from a specific heat analysis<sup>17</sup>. The fact that a mean field law is able to account for the thermal variation of the Gd moment, whereas it fails to reproduce the magnetisation curves (Fig.7, inset), probably stems from the fact that  $M_{\text{Gd}}(T)$  is not very sensitive to the exact shape of  $H_{\text{ex}}(T)$ , and that for  $\text{Gd}^{3+}$  an ionic description is valid.

### C. $^{155}\text{Gd}$ Mössbauer evidence for persisting $T \rightarrow 0$ magnetic fluctuations.

The evidence for the persistence of the magnetic fluctuations is based on the analysis of the relative intensities of the Mössbauer absorption lines of the 27 mK data on Fig.8. We have described this approach previously<sup>24</sup> for the case of the pyrochlore  $\text{Gd}_2\text{Sn}_2\text{O}_7$  and recall the main features. For the values of the saturated magnetic and quadrupole hyperfine interactions established above, the four hyperfine levels of the  $^{155}\text{Gd}$   $I = 3/2$  ground state span an energy range of 20 mK. Below  $\sim 100$  mK, the relative populations of these levels will differ from the equipopulated values that pertain at higher temperatures and this leads to changes in the relative intensities of the absorption lines. By measuring these relative intensities on the low temperature spectrum, it is possible to obtain the effective temperature of the hyperfine levels, which in conventional magnetically ordered magnetic compounds corresponds to the temperature of the sample. We find an effective hyperfine level temperature of 47(8) mK (full line fit on Fig.8) which is significantly higher than the measurement probe temperature (27 mK), *i.e.* the lattice temperature of the sample (dashed line on Fig.8). In other words, the steady state populations of the hyperfine levels are not those corresponding to thermal equilibrium. This indicates that at 27 mK, there is a finite  $\text{Gd}^{3+}$  spin flip time which is of the same magnitude as the nuclear relaxation time. This approach cannot provide quantitative information concerning the rate of the spin fluctuations since the nuclear relaxation time is unknown. We recall that the good quality data fits on Fig.8 were made with the assumption of a “static” hyperfine field, *i.e.* a hyperfine field (or  $\text{Gd}^{3+}$  magnetic moment) which appears static on the scale of the  $^{155}\text{Gd}$  hyperfine Larmor frequency ( $\sim 1.2 \times 10^8 \text{ s}^{-1}$ ). The low temperature  $\text{Gd}^{3+}$  spin fluctuations that are evidenced by the anomalous hyperfine level populations thus occur with frequencies below this value. Since the fluctuations of the  $\text{Gd}^{3+}$  moments are driven by the fluctuations of the  $\text{Mo}^{4+}$  derived exchange field, this shows the correlated moments of the  $\text{Mo}^{4+}$  sublattice also continue to fluctuate at 27 mK.

## V. SUMMARY AND DISCUSSION.

We have studied the pyrochlore compounds  $\text{Yb}_2\text{Mo}_2\text{O}_7$  and  $\text{Gd}_2\text{Mo}_2\text{O}_7$  by microscopic hyperfine techniques ( $^{170}\text{Yb}$ ,  $^{155}\text{Gd}$  Mössbauer and  $^{172}\text{Yb}$  perturbed angular correlation spectroscopies) and bulk magnetic measurements and we have obtained information concerning three aspects of their properties : crystallographic disorder, the magnetic interactions and the role of magnetic frustration.

In  $\text{Yb}_2\text{Mo}_2\text{O}_7$ , the  $\text{Yb}^{3+}$  site symmetry is lower than that of the rare earth site in the standard pyrochlore structure. The distortions are local, since the room tem-



perature X-ray diffraction spectra indicate that the overall cubic lattice symmetry is preserved. In addition, there is considerable lattice disorder. In  $\text{Gd}_2\text{Mo}_2\text{O}_7$ , there is no definite evidence of local symmetry lowering but this cannot be excluded and there is some evidence of local disorder.

In semi-conducting  $\text{Yb}_2\text{Mo}_2\text{O}_7$ , the Mo-Mo exchange coupling is dominated by an interaction which is antiferromagnetic as is the case in semi-conducting  $\text{Y}_2\text{Mo}_2\text{O}_7$ . Based on the analysis of the magnetic susceptibility in the low temperature paramagnetic phase within a molecular field model, the strength of this coupling is of the same order of magnitude as the irreversibility temperature ( $T_{irr} = 17\text{ K}$ ). In this case, the Mo-Mo exchange in  $\text{Yb}_2\text{Mo}_2\text{O}_7$  is much smaller than that in  $\text{Y}_2\text{Mo}_2\text{O}_7$ . It is possible however, that the Mo-Mo coupling is much bigger than that corresponding to  $T_{irr}$ . Additional studies (for example, in field  $^{57}\text{Fe}$  Mössbauer,  $\mu\text{SR}$  or neutron diffraction measurements) are needed to investigate this point. At low temperatures, the  $\text{Yb}^{3+}$  are magnetically polarised by the field coming from the  $\text{Mo}^{4+}$  sublattice. The mean value of the saturated field reaching a  $\text{Yb}^{3+}$  is 3 T and the mean value of the saturated  $\text{Yb}^{3+}$  moment is  $1.7\mu_B$ . In metallic  $\text{Gd}_2\text{Mo}_2\text{O}_7$ , ferromagnetic correlations dominate, as shown by the saturation of the magnetisation at 2 K and by the sharp rise in the susceptibility at 80 K. Below this latter temperature, the  $\text{Gd}^{3+}$  are magnetically polarised by the field coming from the  $\text{Mo}^{4+}$  sublattice and the saturated value of this field is 5.5 T.

In  $\text{Y}_2\text{Mo}_2\text{O}_7$ , Mo spin fluctuations are known to persist as  $T \rightarrow 0$ <sup>15,16</sup>. It seems likely that such fluctuations will also be present in  $\text{Yb}_2\text{Mo}_2\text{O}_7$ . Because the hyperfine fields in  $\text{Yb}_2\text{Mo}_2\text{O}_7$  appear static on the  $^{170}\text{Yb}$  Mössbauer frequency scale of  $\sim 3.0 \times 10^8\text{ s}^{-1}$ , any fluctuations that occur must take place at frequencies that are lower than this value. In  $\text{Gd}_2\text{Mo}_2\text{O}_7$ , we find that  $\text{Gd}^{3+}$  and  $\text{Mo}^{4+}$  spin fluctuations persist as  $T \rightarrow 0$  so evidencing spin liquid behaviour. The continued influence of frustration is somewhat surprising for it concerns a case where the coupling is ferromagnetic and where no important single ion anisotropy is involved. It is possible that the frustration is linked to the role of further neighbour interactions which are antiferromagnetic.

For both a semi-conducting pyrochlore where the dominant Mo-Mo interaction is anti-ferromagnetic ( $\text{Y}_2\text{Mo}_2\text{O}_7$ <sup>15,16</sup>) and a metallic pyrochlore ( $\text{Gd}_2\text{Mo}_2\text{O}_7$ , present results) where the dominant interaction is ferromagnetic, the spin fluctuations persist as  $T \rightarrow 0$ .

- <sup>1</sup> M.A. Subramanian, A.W. Sleight, Handbook on the Physics and Chemistry of Rare Earths **16** (1993) 225, Editors: K.A. Gschneidner Jr., L. Eyring, Elsevier Science Publishers.
- <sup>2</sup> J.E. Greedan, Landolt-Börnstein New Series Group III (Springer Verlag) **27g** 87-123
- <sup>3</sup> H.T. Diep, editor, *Magnetic Systems with Competing Interactions*, (World Scientific, Singapore) (1994)
- <sup>4</sup> R. Moessner, Canadian Journal of Physics **79** (2001) 1283
- <sup>5</sup> See for example, the proceedings of the Waterloo Conference on Highly Frustrated Magnetism: Canadian Journal of Physics **79** (2001) 1283-1596
- <sup>6</sup> J. Villain, Z. Phys. **B 33** (1979) 31
- <sup>7</sup> J.E. Greedan, M. Sato, N. Ali, W.R. Datars, J. Solid State Chem. **68** (1987) 300
- <sup>8</sup> N. Ali, M.P. Hill, S. Labroo, J.E. Greedan, J. Solid State Chem. **83** (1989) 178
- <sup>9</sup> T. Katsufuji, H.Y. Hwang, S-W. Cheong, Phys. Rev. Lett. **B 84** (2000) 1998
- <sup>10</sup> Y. Moritomo, Sh. Xu, A. Machida, T. Katsufuji, E. Nishibori, M. Takata, M. Sakata, S-W. Cheong, Phys. Rev. **B 63** (2001) 144425
- <sup>11</sup> J.E. Greedan, M. Sato, Xu Yan, F.S. Razavi, Solid State Comm. **59** (1986) 895
- <sup>12</sup> J.-S. Kang, Y. Moritomo, Sh. Xu, C.G. Olson, J.H. Park, S.K. Kwon, B.I. Min, Phys. Rev. **B 65** (2002) 224422
- <sup>13</sup> C.H. Booth, J.S. Gardner, G.H. Kwei, R.H. Heffner, F. Bridges, M.A. Subramanian, Phys. Rev. **B 62** (2000) R755
- <sup>14</sup> A. Keren, J.S. Gardner, Phys. Rev. Lett. **87** (2001) 177201
- <sup>15</sup> S.R. Dunsiger et al, Phys. Rev. **B 54** (1996) 9019
- <sup>16</sup> J.S. Gardner, B.D. Gaulin, S.-H. Lee, C. Broholm, N.P. Raju, J.E. Greedan, Phys. Rev. Lett. **83** (1999) 211
- <sup>17</sup> N.P. Raju, E. Gmelin, R.K. Kremer, Phys. Rev. **B 46** (1992) 5405
- <sup>18</sup> H. R. Ott, H. Rudigier, F. Hulliger, Solid State Comm. **55** (1985) 113
- <sup>19</sup> P. Bonville, E. Bauer, J. Phys.: Condens. Matter **8** (1996) 7797
- <sup>20</sup> J.A. Hodges, P. Bonville, A. Forget, M. Rams, K. Królas, G. Dhalenne, J. Phys.: Condens. Matter **13** (2001) 9301
- <sup>21</sup> K. Królas, M. Rams, Hyperfine Interactions **C 1** (1996) 159
- <sup>22</sup> J.D. Cashion, D.B. Browse, A. Vas, J. Phys.C: Solid State Phys. **6** (1973) 2611
- <sup>23</sup> Y. Yasui, Y. Kondo, M. Kanada, M. Ito, H. Harashina, M. Sato, K. Kakurai, J. Phys. Soc. Japan **70** (2001) 284
- <sup>24</sup> effective hyperfine temperature in  $\text{Gd}_2\text{Sn}_2\text{O}_7$  E. Bertin, P. Bonville, J.-P. Bouchaud, J.A. Hodges, J.-P. Sanchez, P. Vulliet, Eur. Phys. J. **B 27** (2002) 347